coatings

MDPI

Article

Effect of Aluminizing on the Oxidation of Inconel 718 and Inconel 738LC Superalloys at 925–1050 °C

Yusuf Burak Telbakiroğlu [1,2,*] and Erkan Konca [3]

[1] Material and Process Department, TRMOTOR Power Systems, Ankara 06800, Türkiye
[2] Graduate School of Natural and Applied Sciences, Atılım University, Ankara 06830, Türkiye
[3] Department of Metallurgical and Materials Engineering, Atılım University, Ankara 06830, Türkiye; erkan.konca@atilim.edu.tr
* Correspondence: burak.telbakiroglu@trmotor.com.tr or yusufburak.telbakiroglu@student.atilim.edu.tr

Abstract

This study was undertaken to investigate the effect of aluminizing on the oxidation of Inconel 718 and Inconel 738LC superalloys. Bare and high-activity chemical vapor deposition (CVD) aluminized Inconel 718 and Inconel 738LC samples were oxidized in air at 925, 1000, and 1050 °C for 200 h. Detailed cross-sectional examinations, elemental analyses, mass change measurements, and X-ray diffraction studies were performed. It was observed that the oxidation resistances of both alloys were significantly improved by the Al_2O_3 scale formed on the NiAl layer that was created on the surfaces of the samples during aluminizing. The beneficial effect of aluminizing was found to be more evident in the case of Inconel 738LC alloy samples which showed lower oxidation rates at all test temperatures. The results have been discussed on the basis of the differences in aluminum contents of the alloys and their effects on diffusion.

Keywords: oxidation; superalloy; aluminizing; Inconel 718; Inconel 738; NiAl

check for updates

Academic Editor: Raul Arrabal

Received: 9 November 2025
Revised: 5 December 2025
Accepted: 8 December 2025
Published: 16 December 2025

Citation: Telbakiroğlu, Y.B.; Konca, E. Effect of Aluminizing on the Oxidation of Inconel 718 and Inconel 738LC Superalloys at 925–1050 °C. *Coatings* **2025**, *15*, 1482. https://doi.org/10.3390/coatings15121482

Copyright: © 2025 by the authors. Licensee MDPI, Basel, Switzerland. This article is an open access article distributed under the terms and conditions of the Creative Commons Attribution (CC BY) license (https://creativecommons.org/licenses/by/4.0/).

1. Introduction

Nickel-based superalloys, such as Inconel 718 and Inconel 738, are favorable groups of materials for high-temperature applications such as gas turbine blades, discs, shafts, etc., due to their unique combination of high strength, fatigue, creep, oxidation and corrosion properties [1,2]. Although they are highly resistant to oxidation and corrosion, there is a certain upper temperature limit for the usage of these materials. It is a never-ending desire to increase the service temperatures of these alloys which benefits from higher oxidation resistance. Aluminizing is one of the ways of increasing the oxidation resistance of nickel-based superalloys by forming a β-NiAl layer on their surfaces [3,4]. When exposed to high-temperature, this β-NiAl layer gets oxidized to form an Al_2O_3 scale in which diffusivity of oxygen is very low [5]. By this way, penetration of oxygen into the nickel-based superalloy substrate is slowed and hence its service life is improved. In the literature, there are various methods to produce an aluminide coating such as pack aluminizing [6], high and low activity aluminizing by chemical vapor deposition [3,4], slurry aluminizing [7] and hot-dip aluminizing [8]. Each method produces different microstructures with characteristic properties which affect the service life of the substrate significantly.

The beneficial effects of pack and hot-dip aluminizing methods on the oxidation of Inconel 718 and 738 alloys were previously studied. Kalaycı investigated the isothermal oxidation performance of hot dip aluminized Inconel 718 at 1000 °C for 1, 6, 48, 192, and

336 h. It was observed that Inconel 718 with an Al_2O_3 scale showed better oxidation resistance compared to Inconel 718 with a Cr_2O_3 scale [9]. In the case of Inconel 738, Bai et al. studied the isothermal oxidation performance of aluminized Inconel 738LC samples by pack cementation method at 850, 1000, 1100, and 1200 °C for 288 h. It was observed that aluminized Inconel 738LC samples showed better oxidation resistance even at 1100 °C [10].

Compared with conventional pack or hot-dip aluminizing, high/low-activity CVD aluminizing provides superior control over Al activity, enabling the formation of a uniform and compositionally precise NiAl diffusion layer. This method produces a cleaner coating without halide residues, offers better thickness controllability, and results in a more adherent β-NiAl layer with reduced porosity and improved oxidation resistance.

As presented above, while there are several studies on the oxidation behavior of pack and hot-dip aluminized Inconel 718 and Inconel 738 alloys, investigations on the CVD aluminized samples are extremely limited. With this motivation, the current study focuses on the effect of high activity CVD aluminizing on the oxidation resistances of Inconel 718 and Inconel 738LC superalloys within the temperature range of 925–1050 °C, which is conventionally considered above the typical service temperatures of these alloys. It is of interest to see how these two different alloys would respond to oxidation after being aluminized under the same conditions so that the role of substrate composition on the oxidation resistance can be delineated. To the best of authors' knowledge, there is no study in open literature where the oxidation behavior of bare and high-activity CVD-aluminized Inconel 718 and Inconel 738LC alloys were investigated and compared under such conditions.

2. Experimental

2.1. Materials

The chemical compositions of the Inconel 718 and Inconel 738LC samples are given in Table 1. Inconel 718 samples were procured from Enpar Sonderwerkstoffe GmbH (Gummersbach, Germany) with AMS 5662 specification [11]. Inconel 738LC samples were supplied by Ross & Catherall Ltd. (Sheffield, UK). The samples were 12.7 mm in diameter and 7–10 mm in height.

Table 1. Chemical compositions of the superalloy substrates (wt. %).

Material	Fe	Cr	Nb	Mo	Ti	Al	Co	W	C	Ni
Inconel 718	17.72	19.21	5.28	2.98	0.96	0.49	0.38	-	0.03	52.95
Inconel 738LC	-	15.95	0.86	-	3.45	3.43	8.40	2.57	0.14	65.20

High-activity CVD aluminizing of the samples was performed at the Critical Metallic Materials Unit of TUBITAK Marmara Research Center (Gebze, Kocaeli Turkiye). A %50Al-%50Cr ingot was used as the Al source. The aluminizing process was carried out at 1070 °C for 4 h. After aluminizing, the samples were heat treated at 1070 °C for 2 h under an inert atmosphere of argon. Cross-sectional examination of the as-aluminized samples, presented in the Results section, showed that the average thickness of the aluminized layer is about 24.5 ± 0.5 μm.

2.2. Oxidation Tests

Isothermal oxidation tests shown in Table 2 were conducted using a Protherm PLF 110/30 furnace (Alser Teknik, Ankara, Türkiye) at the Heat Treatment Laboratory of the Metallurgical and Materials Engineering Department of Atılım University (Ankara,

Türkiye). Aluminized samples were tested at 925, 1000, and 1050 °C, while the bare samples were tested only at 925 and 1050 °C. Duration of the oxidation tests was 200 h for all samples. An exposure duration of 200 h was selected as the most critical oxidation mechanisms in aluminized Ni-based coatings such as α-Al_2O_3 scale formation and early Al depletion occur within this timeframe. Beyond 200 h, oxidation generally approaches a steady state and provides limited additional insight for comparative evaluation. Thus, 200 h represents an effective and widely used benchmark for mid-term oxidation performance. In each test, the sample was placed in the furnace at room temperature to prevent any thermal shock which may cause spallation and failure of the coating due to rapid thermal expansion during heating. The average heating rate to the test temperature was 5 °C/min for all samples. At the end of each oxidation test, the power of the furnace was cut off to cool down the furnace to the room temperature before the sample was taken out. Temperature in the furnace was tracked and recorded by Ordel DaLi 08 software (Ankara, Turkey).

Table 2. Experimental Conditions.

	Oxidation Test Temperature (°C)		
Sample	**925**	**1000**	**1050**
Bare 718	✓	-	✓
Bare 738LC	✓	-	✓
Aluminized 718	✓	✓	✓
Aluminized 738LC	✓	✓	✓
All samples were tested for 200 h.			

2.3. Characterization of the Samples

All weighing operations were performed using a Denver Instrument TP-214 precision balance, which provides a readability of 0.1 mg, a repeatability better than ±0.1 mg, and a linearity of ±0.2 mg. Cross-sectional examinations of the samples were performed using a Carl Zeiss Merlin field emission scanning electron microscope (FESEM) located in Atılım University Metal Forming Center of Excellence (Ankara, Turkey). EDAX energy-dispersive spectroscope (EDS) detector was used for chemical identification. Rigaku DMAX 2200 X-ray diffractometer was used with Cu-Kα radiation (λ = 0.15406 nm) for the phase identification of the samples. Scan speed was set to 1°/min. The XRD patterns were analyzed by using Match! (Bonn, Germany) version 4.6 software [12].

3. Results

Results of the oxidation tests of bare samples are given in Table 3. At 950 °C, the Inconel 718 sample experienced a weight gain of 8.5 g/m^2 and that of the Inconel 738LC sample was 12.1 g/m^2. However, increasing the oxidation temperature to 1050 °C reversed the weight gains into significant weight losses for both samples. The Inconel 718 sample suffered a weight loss of 54.2 g/m^2, while the loss of Inconel 738LC sample was 35.6 g/m^2. The fact that the weight change values became negative after testing at 1050 °C indicates evaporative loss to be discussed later in Section 4.1.

Table 3. Oxidation test results of the bare samples.

Sample	Weight Change (g/m^2)	Rate of Weight Change (g/m^2.h)
Bare 718-925 °C	8.5	0.043
Bare 738LC-925 °C	12.1	0.061
Bare 718-1050 °C	−54.2	−0.271
Bare 738LC-1050 °C	−35.6	−0.178

A cross-sectional SEM image of the bare Inconel 718 sample oxidized at 925 °C is given in Figure 1a. A non-uniform and cracked NiO layer was detected at the top of the sample. The average thickness of this layer is 3.4 µm. A Fe-Ni oxide with a thickness of 5.0 µm was formed under the NiO layer. Cr_2O_3 layer was observed under the Fe-Ni oxide. The average thickness of the Cr_2O_3 layer is 6.3 µm. Ni-Nb oxide formed under the Cr_2O_3 layer at some regions. In addition to the oxides formed on the top, internal oxidation of Ti-Ni-Cr-Al is also observed in this sample. The average depth of internal oxidation reached to 9.30 µm.

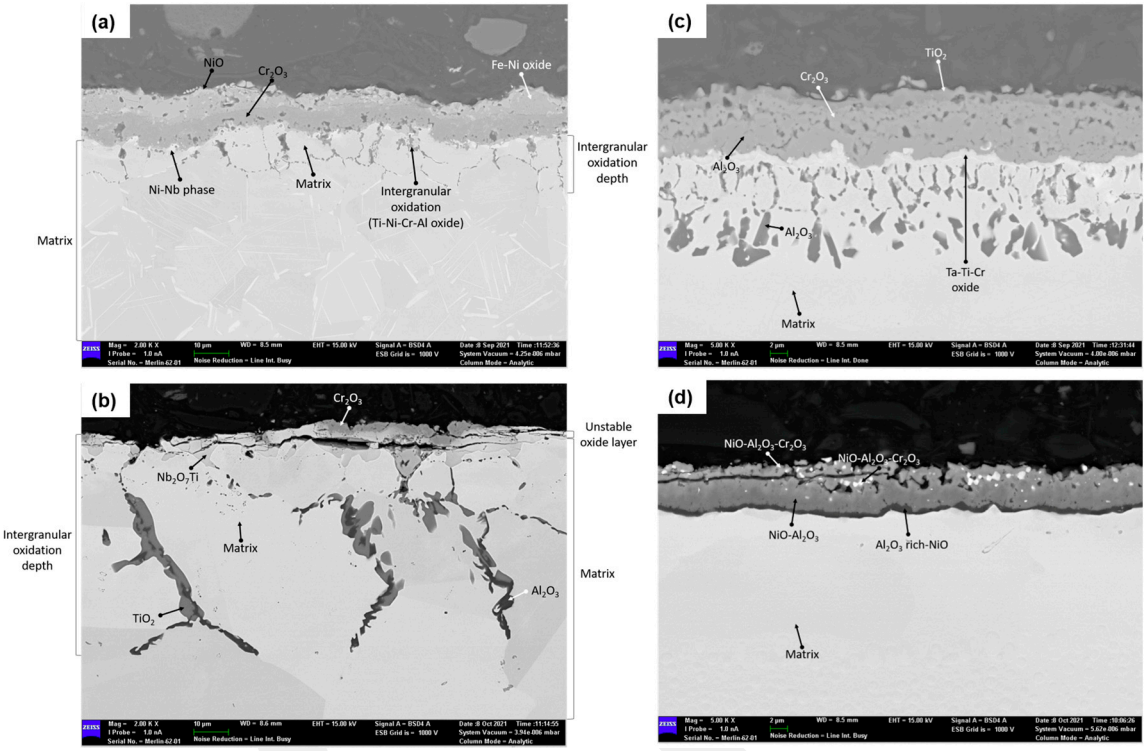

Figure 1. Cross-sectional SEM images of oxidized bare Inconel samples (**a**) 718 at 925 °C, (**b**) 718 at 1050 °C, (**c**) 738LC at 925 °C, (**d**) 738LC at 1050 °C. The EDS data used for phase identification is presented in Tables A1 and A2.

A cross-sectional SEM image of the bare 718 sample oxidized at 1050 °C is given in Figure 1b. A non-uniform oxide layer was observed on the top. The formed scale, mainly Cr_2O_3, was cracked, delaminated, and discontinuous. In addition to Cr_2O_3, Nb_2O_7Ti is also observed at the top region. Intergranular oxidation occurred under these surface oxides. Main products of intergranular oxidation are determined to be TiO_2 and Al_2O_3. The average depth of internal oxidation in this sample was 55.45 µm, which is significantly deeper than the value for the sample tested at 925 °C (9.30 µm).

In Figure 1c, a cross-sectional SEM image of bare Inconel 738LC sample oxidized at 925 °C is given. The very top layer consists of TiO_2 while Cr_2O_3 and Al_2O_3 are present under this layer. This is followed by oxides of Ta-Ti-Cr. Also, formation of islands of Al_2O_3, i.e., internal oxidation, is observed to a significant degree in the matrix.

The cross-sectional SEM image of the bare Inconel 738LC sample oxidized at 1050 °C (Figure 1d) was quite different than that oxidized at 925 °C. First of all, the overall thickness of the oxidized region was thinner. At the top layer, $NiO\text{-}Al_2O_3\text{-}Cr_2O_3$ was formed. A $NiO\text{-}Al_2O_3$ layer was observed under this layer where the Al content (hence the Al_2O_3) increased with depth. Different than the 925 °C test, no islands of Al_2O_3 formed at 1050 °C.

Results of the oxidation tests of aluminized samples are given in Table 4. For the aluminized Inconel 718 samples, the weight gain after 200 h of oxidation was 5.0 g/m^2

at 925 °C, 6.6 g/m^2 at 1000 °C, and it was 6.8 g/m^2 at 1050 °C. Noticeably lower weight gains were measured in the case of aluminized Inconel 738LC samples; it was 3.1 g/m^2 after testing at 925 °C, 3.7 g/m^2 at 1000 °C and 4.5 g/m^2 at 1050 °C. Comparison of the weight change values of bare vs. aluminized samples (Table 3 vs. Table 4) clearly shows that aluminizing is very effective in protecting the Inconel substrates.

Table 4. Oxidation test results of the aluminized samples.

Sample	Weight Change (g/m^2)	Rate of Weight Change (g/m^2.h)
Alum-718-925 °C	5.0	0.025
Alum-718-1000 °C	6.6	0.033
Alum-718-1050 °C	6.8	0.034
Alum-738LC-925 °C	3.1	0.016
Alum-738LC-1000 °C	3.7	0.019
Alum-738LC-1050 °C	4.5	0.023

The XRD patterns of the aluminized samples are given in Figure 2. The presence of β-NiAl (PDF 33-0948) phase is confirmed for both series of samples when compared with reference B-NiAl [13].

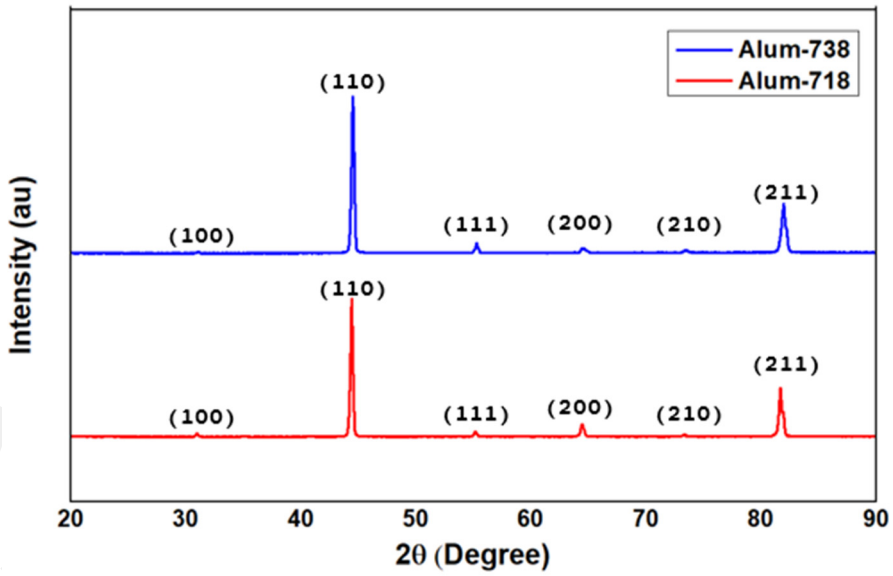

Figure 2. XRD patterns of the aluminized samples before the oxidation tests. All peaks belong to β-NiAl.

A cross-sectional SEM image of the aluminized 718 sample before an oxidation test (i.e., in as-aluminized condition) is given in Figure 3a. At the top surface, β-NiAl phase was observed. The average thickness of the β-NiAl layer is 25.4 µm. An interdiffusion zone (IDZ) with a thickness of 11.9 µm was detected under the β-NiAl layer. Nb-Fe-Cr-Ni and Cr-Fe-Ni-Mo phases were present at IDZ.

In Figure 3b, a cross-sectional image of the as-aluminized 738LC sample can be seen. At the top, β-NiAl phase with a thickness of 24.2 µm was formed. Again an IDZ was formed under the β-NiAl layer. Average thickness of IDZ is about 16.8 µm. There were three different microstructural constituents in the IDZ of this sample: Ta-Ti-Nb-W carbides, β-NiAl, and Cr-Ni-Co-W phases.

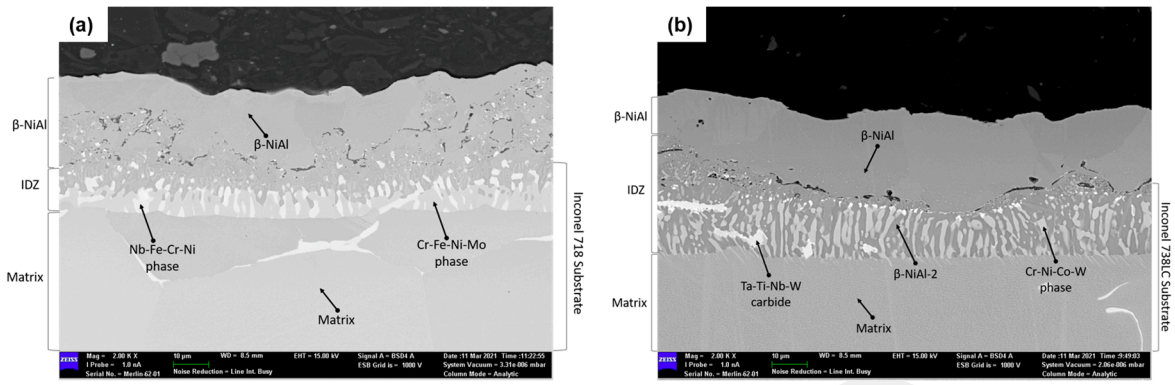

Figure 3. Cross-sectional SEM images of the aluminized Inconel samples before oxidation tests (**a**) 718 (**b**) 738LC. The EDS data used for phase identification is presented in Tables A3 and A4.

The XRD patterns of the aluminized samples oxidized at 1000 °C are given in Figure 4. As expected, the peaks were dominantly from the α-Al_2O_3 (PDF 46-1212) [14] scale formed during oxidation. In addition, some NiAl peaks were also observed.

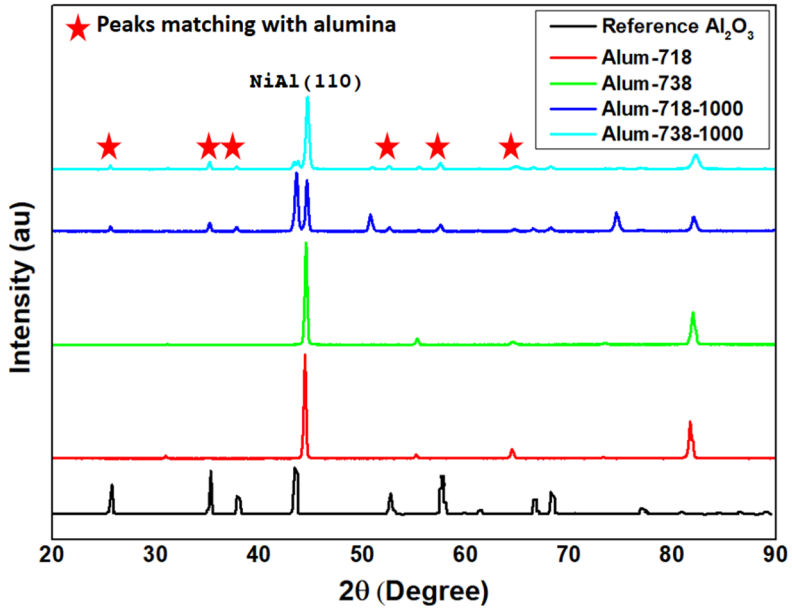

Figure 4. XRD patterns of the aluminized 718 and 738 samples after the oxidation tests (Cu K-α).

A cross-sectional SEM image of the aluminized 718 sample which was oxidized at 925 °C can be seen in Figure 5a. An Al_2O_3 scale with an average thickness of 2.8 μm was formed. β-NiAl layer with an average thickness of 18.49 μm comes under the Al_2O_3 scale. A Cr-Fe-Ni-Mo region was formed under the β-NiAl layer. The average thickness of Cr-Fe-Ni-Mo region was 7.4 μm. Nb-Cr-Mo-Ni particles were observed between the Cr-Fe-Ni-Mo and β-NiAl regions.

Figure 5b shows the cross-sectional SEM image of the aluminized 718 sample oxidized at 1000 °C. At the top a thicker Al_2O_3 scale with an average thickness 3.6 μm was formed. There were some cracks and voids in this layer. β-NiAl and other Ni-rich phases were observed under the Al_2O_3 scale. Nb-Mo-Cr particles were formed under the Ni-rich and β-NiAl phases.

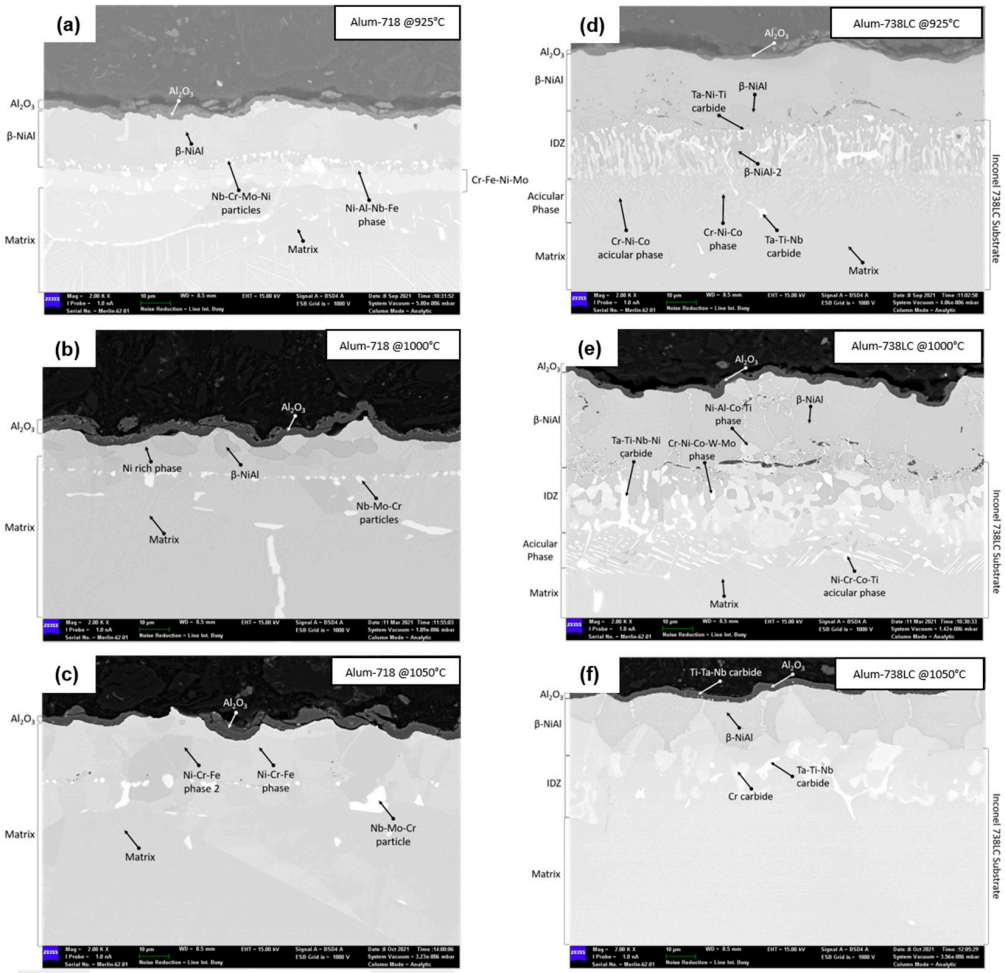

Figure 5. Cross-sectional SEM images of the aluminized Inconel samples after oxidation tests: (**a**) Alum-718 at 925 °C, (**b**) Alum-718 at 1000 °C, (**c**) Alum-718 at 1050 °C, (**d**) Alum-738LC at 925 °C, (**e**) Alum-738LC at 1000 °C, and (**f**) Alum-738LC at 1050 °C. The EDS data used for phase identification is presented in Tables A5–A10.

In Figure 5c, a cross-sectional SEM image of the aluminized 718 sample oxidized at 1050 °C is given. At the top Al_2O_3 partially covered the surface. The Al_2O_3 scale had many cracks and separated parts. The average thickness of Al_2O_3 layer was 3.3 µm. There were Ni-Cr-Fe phases under the Al_2O_3 layer. Also, some Nb-Mo-Cr particles are observed at regions close to the surface.

A cross-sectional SEM image of the aluminized 738LC sample which was oxidized at 925 °C can be seen in Figure 5d. At the top, an Al_2O_3 layer was formed. Average thickness of the Al_2O_3 layer is 2.1 µm. Under the Al_2O_3 layer, a β-NiAl layer with a thickness of about 24.5 µm was present. Ta-Ni-Ti carbides were formed between β-NiAl and IDZ. Under the Ta-Ni-Ti carbides, IDZ can be observed. IDZ mainly consisted of β-NiAl phase. Average thickness of IDZ is 15.5 µm. A Cr-Ni-Co acicular phase with a thickness of 11.4 µm was formed under the IDZ. Ta-Ti-Nb carbides were observed in the acicular phase region.

A cross-sectional SEM image of the aluminized 738LC sample oxidized at 1000 °C is seen in Figure 5e. An Al_2O_3 layer with an average thickness of 2.2 µm was formed at the top. Under the Al_2O_3 layer, β-NiAl layer with a thickness of 28.1 µm was observed. IDZ was observed under the β-NiAl layer. The average thickness of IDZ is 20.1 µm. Ni-Al-Co-Ti phase was seen between the β-NiAl and IDZ. In IDZ, Ta-Ti-Nb-Ni carbides and Cr-Ni-Co-W

phases were observed. Under the IDZ, acicular Ni-Cr-Co-Ti region with a thickness of 9.8 μm was seen.

Finally, an SEM image of the aluminized 738LC sample oxidized at 1050 °C is given in Figure 5f. As in all tested aluminized samples, an Al_2O_3 layer was formed at the top. Average thickness of the Al_2O_3 layer is 2.0 μm. Under the Al_2O_3 layer, a partial covering β-NiAl layer with a thickness of 12.9 μm was observed. Ti-Ta-Nb carbides were seen between the Al_2O_3 and β-NiAl layers. IDZ formed under the β-NiAl layer. The average thickness of IDZ is 17.6 μm. Two different carbides formed in the IDZ as Cr carbide and Ta-Ti-Nb carbide.

One general observation for all aluminized samples is the fact that they did not suffer from internal oxidation as some of the bare samples did.

4. Discussion

4.1. Effect of Aluminizing on the Oxidation Behavior Inconel 718 and 738LC

As shown in Table 3, the weight changes were negative for the bare Inconel 718 and 738LC samples oxidized at 1050 °C. A plausible explanation for the negative weight change is the reaction of Cr_2O_3 that forms on the top surface with oxygen to produce volatile CrO_3 at temperatures greater than 1000 °C [15]. In order to be able to compare the results obtained at different temperatures, a calculation was performed where it is assumed that all of the mass losses of the bare samples at 1050 °C are due to the evaporated Cr, and this amount is converted to Cr_2O_3 and added into to the final weight of the samples as if Cr_2O_3 was present on their surfaces. As a result, the value of −0.271 g/m^2.h became +0.355 g/m^2.h for the bare 718-1050 sample and the value of −0.178 g/m^2.h became +0.251 g/m^2.h for the bare 738LC sample (Table 5). It should be noted that this calculation is just an approximation, as the final weights of the 1050 °C samples already include some oxides indicating that the actual Cr loss in these samples is higher than what is assumed here.

Table 5. Recalculation of the weight changes in bare samples tested at 1050 °C.

	Actual Measurement		**Recalculated After Cr Loss was Incorporated as Cr_2O_3**	
Sample	**Weight Change (g/m^2)**	**Rate of Weight Change (g/m^2.h)**	**Weight Change (g/m^2)**	**Rate of Weight Change (g/m^2.h)**
Bare 718-1050 °C	−54.2	−0.271	+70.9	+0.355
Bare 738LC-1050 °C	−35.6	−0.178	+50.2	+0.251

Oxidation rates of the bare and aluminized samples are plotted in Figure 6. It is seen that the relative effectiveness of aluminizing on preventing oxidation becomes more critical with increasing test temperature from 925 °C to 1050 °C. Already at 925 °C aluminizing decreases the oxidation rate of Inconel 718 by 42% (0.043 g/m^2.h for bare 718 vs. 0.025 g/m^2.h for aluminized) while the decrease in oxidation rate reaches to 90% at 1050 °C (0.355 g/m^2.h for bare vs. 0.034 g/m^2.h for aluminized). Similarly, with respect to the bare sample the oxidation rate of the aluminized 738LC sample was 74% lower at 925 °C (0.061 g/m^2.h for bare vs. 0.016 g/m^2.h for aluminized) and it was 91% lower at 1050 °C (0.251 g/m^2.h for bare vs. 0.023 g/m^2.h for aluminized).

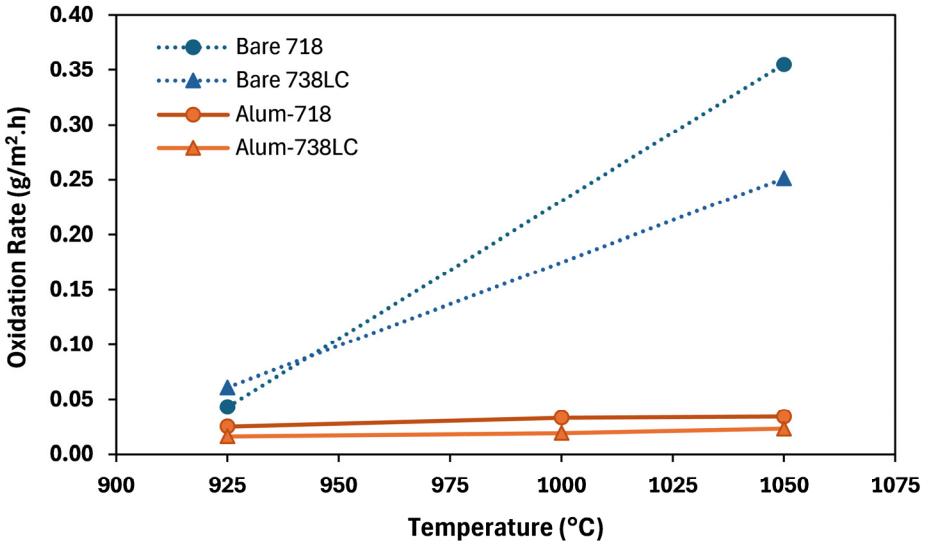

Figure 6. Oxidation rate versus test temperature for the bare and aluminized samples.

4.2. Role of Substrate Alloy Composition on the Oxidation Behavior

The clear difference in the oxidation rates of the aluminized samples suggests that substrate composition still plays a significant role in oxidation behavior. The improved oxidation resistance of aluminized samples is due to the very low diffusion coefficient of oxygen in Al_2O_3 scale [5] that forms at the top surface as a partial conversion from the NiAl layer. Therefore, the survival of the Al_2O_3 layer is very critical for the sustainability of protection from further oxidation. The Al_2O_3 layer is backed by the NiAl layer which serves as the aluminum source to form Al_2O_3. This means that the longevity of the Al_2O_3 layer is essentially dependent on the life of the NiAl layer backing it. The life of the NiAl layer, in turn, must be primarily dependent on the substrate composition together with other factors.

During the oxidation tests, while some aluminum of the NiAl layer is consumed by the formation of Al_2O_3 at the top surface (i.e., oxidational loss) there is also a simultaneous consumption of aluminum from the other end of the NiAl layer into the substrate through IDZ (i.e., diffusional loss) as depicted in Figure 7. Therefore, the NiAl layer is simultaneously consumed from both ends at high temperatures.

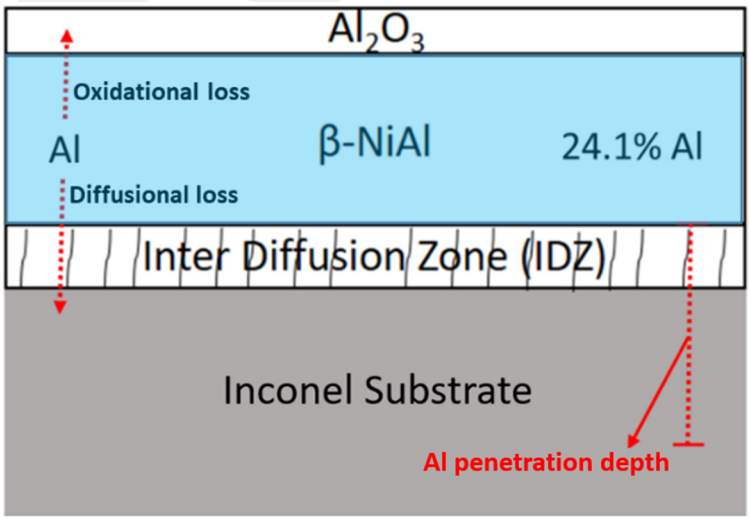

Figure 7. Schematic illustration of the mechanisms of aluminum loss from the NiAl layer.

It is suggested that the difference in the aluminum contents of the two base alloys is the primary reason for the difference in their oxidation rates observed in this study. The aluminum content of Inconel 718 is 0.49%, whereas that of Inconel 738LC is 3.43% (Table 1). The aluminum content of the NiAl layer formed during aluminizing is about 24.1 wt.% as determined by EDS analysis. Therefore, as compared to the case of aluminized Inconel 738LC, a much steeper aluminum concentration gradient develops in the case of Inconel 718 after aluminizing. This steeper Al concentration gradient in Inconel 718 results in a higher diffusional flux of aluminum atoms away from the NiAl layer down into the substrate. As a result, the NiAl layer is consumed more quickly in the case of Inconel 718, leading to its relatively poorer resistance against oxidation. The criticalness of the diffusional loss of Al causing the degradation of the aluminide layer is also emphasized in a recent study by Sarraf et al. [16].

In order to evaluate this idea, EDS line analyses of the cross-sections of the as-aluminized and 1050 °C oxidized aluminized samples were obtained. It is observed that the depth of penetration of Al from the NiAl layer into the substrate reaches to about 135 µm after testing at 1050 °C for 200 h for the Alum-718-1050 °C sample as shown in Figure 8. On the other hand, the depth of penetration of Al into the Alum-738LC substrate tested under the same conditions is about 100 µm which is significantly shorter (Figure 9). Comparison of the EDS line analyses of the two series of samples tested at other temperatures also yields similar results as given in Table 6. This table shows that while increasing the test temperature increases the depth of penetration of aluminum for both series of samples, aluminum penetration is consistently deeper in the case of Inconel 718. It is clear that the NiAl layer of Inconel 718 suffered much higher loss of Al due to its lower base Al content of 0.49 wt.% as compared to the 3.43 wt.% Al of Inconel 738LC.

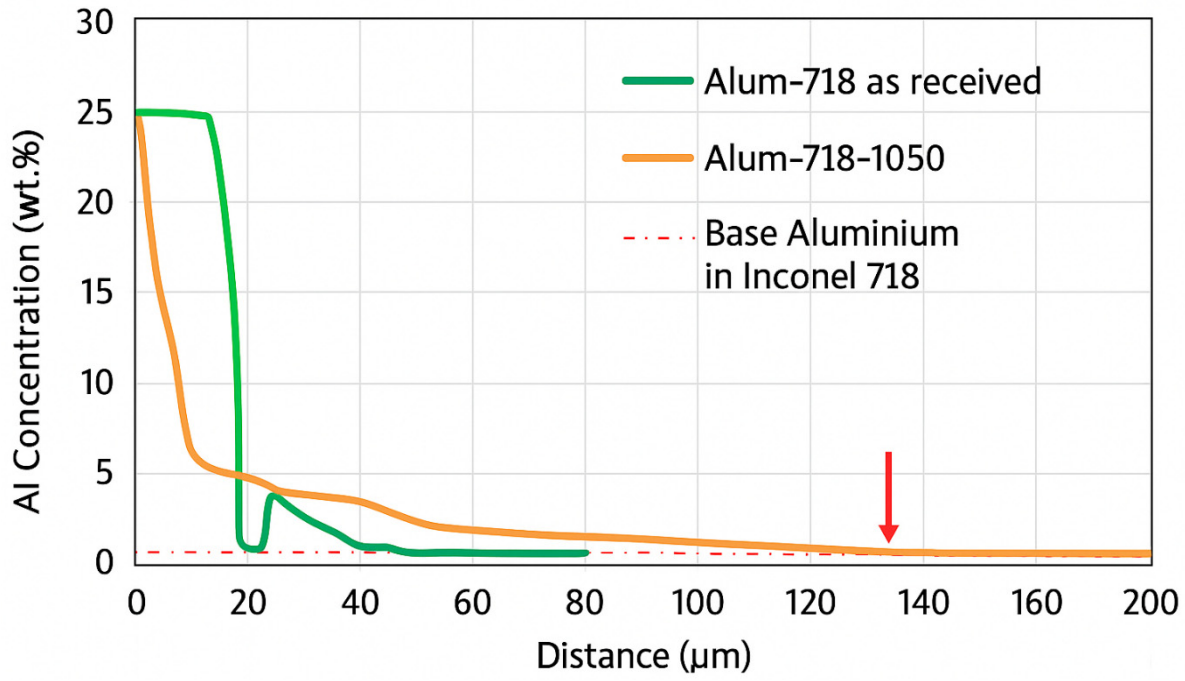

Figure 8. Al depth profiles of the aluminized Inconel 718 samples in as-received and oxidized at 1050 °C conditions. Arrow shows the maximum depth of penetration of aluminum into the substrate by diffusion.

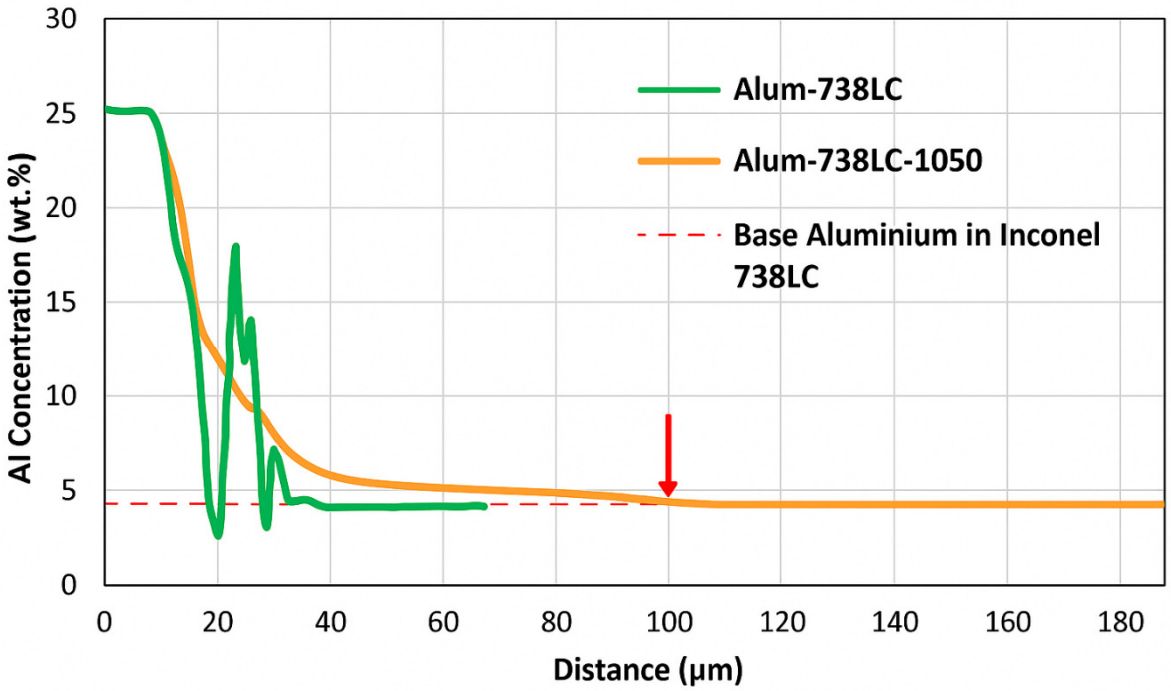

Figure 9. Al depth profiles of the aluminized Inconel 738LC samples in as-received and oxidized at 1050 °C conditions. Arrow shows the maximum depth of penetration of aluminum into the substrate by diffusion.

Table 6. Distance from the bottom of NiAl layer to reach down to the base Al concentration of the substrate alloy.

	Aluminum Penetration Depth (μm)	
Sample	**Inconel 718**	**Inconel 738LC**
As-aluminized	34	23
Tested at 925 °C	65	50
Tested at 1000 °C	100	70
Tested at 1050 °C	135	100

5. Conclusions

Bare and high activity CVD aluminized Inconel 718 and Inconel 738LC samples were oxidized in air at 925, 1000, and 1050 °C for 200 h. It is found that

- Aluminizing drastically improves the oxidation resistance of both alloys where the oxidation rate of aluminized Inconel 738LC is significantly less than that of aluminized Inconel 718 at all temperatures. This suggests that chemical composition of the substrate still plays a critical role in the oxidation behavior of the aluminized samples.
- Aluminizing eliminated the internal oxidation observed in the bare samples.
- The aluminide layer on the Inconel 718 sample was totally consumed above 925 °C. For the aluminized Inconel 738LC samples, although it is partially consumed, the NiAl layer was still present even at 1050 °C.
- It is suggested that the higher aluminum content of Inconel 738LC (3.43 wt.% vs. 0.49 wt.% in Inconel 718) causes less diffusional loss of Al from the NiAl layer to the substrate, which increases the longevity of this layer, resulting in a superior oxidation resistance for this alloy.

Author Contributions: Conceptualization, Y.B.T. and E.K.; methodology, Y.B.T. and E.K.; investigation, Y.B.T.; resources, Y.B.T.; writing—original draft preparation, Y.B.T.; writing—review and editing, Y.B.T. and E.K.; visualization, Y.B.T. and E.K.; supervision, E.K. All authors have read and agreed to the published version of the manuscript.

Funding: This reserach received no external funding.

Institutional Review Board Statement: Not applicable.

Informed Consent Statement: Not applicable.

Data Availability Statement: The original contributions presented in this study are included in the article. Further inquiries can be directed to the corresponding author.

Acknowledgments: The authors are thankful to Havva Kazdal Zeytin, Gökhan Güven, and Kaan Demiralay of TUBITAK MAM Critical Metallic Materials Unit for the provision of the samples. Yusuf Burak Telbakiroğlu is thankful to TRMOTOR Power Systems for supporting his academic studies.

Conflicts of Interest: Authors declare no conflict of interest.

Appendix A

Table A1. EDS analyses of some regions of the bare Inconel 718 sample oxidized at 925 °C (Figure 1a).

Region	Chemical Composition (Weight %)											
	Ni	Cr	Ti	Nb	Al	Fe	Mo	Co	Si	N	O	C
NiO	71.9	1.1	-	-	-	3.4	-	-	-	-	23.6	-
Fe-Ni oxide	20.0	18.8	1.3	0.9	0.8	26.3	-	-	0.2	-	31.7	-
Cr_2O_3	1.0	65.0	1.9	0.7	0.2	-	-	-	0.1	-	31.1	-
Ni-Nb phase	65.0	3.0	-	24.0	-	4.0	3.0	1.0	-	-	-	-
Intergranular oxidation	12.3	11.5	29.0	2.7	9.1	6.0	0.7	0.1	-	1.1	27.5	-
NbC	1.6	-	5.5	76.1	-	-	-	-	-	-	-	16.8
TiN	-	-	69.5	5.6	-	-	-	-	-	22.1	-	2.8
Matrix	58.0	12.6	-	3.3	-	22.6	3.2	0.3	-	-	-	-

Table A2. EDS analyses of some regions of the bare Inconel 718 sample oxidized at 1050 °C (Figure 1b).

Region	Chemical Composition (Weight %)											
	Ni	Cr	Ti	Nb	Al	Fe	Mo	Co	Si	N	O	C
Cr_2O_3	-	61.5	1.4	1.0	0.7	2.0	-	-	-	-	33.4	-
TiO_2	1.1	0.5	61.8	-	1.3	-	-	-	-	3.8	31.5	-
Al_2O_3	4.1	1.7	-	-	53.7	2.0	-	-	-	-	38.5	-
Nb_2O_7Ti	-	6.2	11.9	52.4	-	-	-	-	-	-	29.5	-
Matrix	61.1	11.6	0.2	3.0	-	21.1	3.0	-	-	-	-	-

Table A3. EDS analyses of some regions of the aluminized Inconel 718 sample (Figure 3a).

Region	Chemical Composition (Weight %)											
	Ni	Cr	Ti	Nb	Al	Fe	Mo	Co	Si	N	O	C
β-NiAl	64.5	3.5	-	-	24.1	7.9	-	-	-	-	-	-
Nb-Fe-Cr-Ni phase	16.3	19.1	0.6	31.5	1.1	22.1	8.7	-	0.6	-	-	-

Table A3. *Cont.*

Region	Chemical Composition (Weight %)											
	Ni	**Cr**	**Ti**	**Nb**	**Al**	**Fe**	**Mo**	**Co**	**Si**	**N**	**O**	**C**
Cr-Fe-Ni-Mo phase	16.2	46.6	0.4	2.9	0.8	26.3	6.8	-	-	-	-	-
Matrix	52.5	20.5	1.1	4.6	0.5	18.5	2.3	-	-	-	-	-

Table A4. EDS analyses of some regions of the aluminized Inconel 738LC sample (Figure 3b).

Region	Chemical Composition (Weight %)												
	Ni	**Cr**	**Ti**	**Nb**	**Al**	**Fe**	**W**	**Mo**	**Co**	**Ta**	**N**	**O**	**C**
β-NiAl	65.9	4.2	0.7	-	23.6	-	-	-	5.6	-	-	-	-
β-NiAl-2	64.2	5.9	4.7	-	18.2	-	-	-	7.0	-	-	-	-
Ta-Ti-Nb-W carbide	2.2	2.2	26.4	13.4	-	-	8.0	3.6	-	30.5	-	-	13.7
Cr-Ni-Co-W phase	19.1	50.2	0.8	-	0.8	-	9.4	6.9	12.8	-	-	-	-
Matrix	67.1	14.6	4.2	0.5	3.8	-	1.3	1.1	7.2	0.2	-	-	-

Table A5. EDS analyses of some regions of the aluminized Inconel 718 sample oxidized at 925 °C (Figure 5a).

Region	Chemical Composition (Weight %)												
	Ni	**Cr**	**Ti**	**Nb**	**Al**	**Fe**	**Mo**	**Mn**	**Co**	**Si**	**N**	**O**	**C**
Al_2O_3	-	1.1	2.9	1.9	46.1	-	-	-	-	-	-	48.0	-
B-NiAl	66.9	3.8	0.6	0.6	18.2	9.3	-	0.2	0.4	-	-	-	-
Nb-Cr-Mo-Ni particles	8.7	17.1	0.1	41.2	2.8	4.8	19.1	0.5	0.4	-	-	-	5.3
Ni-Al-Nb-Fe phase	72.7	3.6	1.4	6.7	9.0	6.6	-	-	-	-	-	-	-
Cr-Fe-Ni-Mo phase	18.5	47.9	0.2	1.8	0.4	23.4	7.4	-	0.2	0.2	-	-	-
Matrix	59.6	14.0	1.6	4.4	4.9	14.8	0.7	-	-	-	-	-	-

Table A6. EDS analyses of some regions of the aluminized Inconel 718 sample oxidized at 1000 °C (Figure 5b).

Region	Chemical Composition (Weight %)												
	Ni	**Cr**	**Ti**	**Nb**	**Al**	**Fe**	**Mo**	**Mn**	**Co**	**Si**	**N**	**O**	**C**
Al_2O_3	0.8	1.0	3.2	3.3	49.8	-	0.1	-	-	-	-	41.8	-
B-NiAl	67.4	4.0	0.8	0.5	18.3	8.8	0.2	-	-	-	-	-	-
Ni-rich phase	74.3	3.0	1.9	5.7	9.2	5.6	0.3	-	-	-	-	-	-
Nb-Mo-Cr particles	2.3	19.6	-	48.1	-	4.6	25.4	-	-	-	-	-	-
Nb rich particles	-	-	5.6	94.4	-	-	-	-	-	-	-	-	-
Matrix	52.6	20.6	0.8	3.1	3.0	17.9	2.0	-	-	-	-	-	-

Table A7. EDS analyses of some regions of the aluminized Inconel 718 sample oxidized at 1050 °C (Figure 5c).

Region	Chemical Composition (Weight %)												
	Ni	**Cr**	**Ti**	**Nb**	**Al**	**Fe**	**Mo**	**Mn**	**Co**	**Si**	**N**	**O**	**C**
Al_2O_3	-	0.3	1.3	0.8	53.9	-	-	-	-	-	-	43.7	-
Ni-Cr-Fe phase	47.9	24.9	0.9	2.9	3.3	16.5	3.6	-	-	-	-	-	-
Ni-Cr-Fe-2 phase	58.4	16.1	0.9	3.4	4.6	15.1	1.5	-	-	-	-	-	-
Nb-Mo-Cr particle	2.4	19.9	-	39.4	-	3.9	34.4	-	-	-	-	-	-
Matrix	58.3	16.3	1.0	3.8	4.4	14.5	1.7	-	-	-	-	-	-

Table A8. EDS analyses of some regions of the aluminized Inconel 738LC sample oxidized at 925 °C (Figure 5d).

Region	Chemical Composition (Weight %)												
	Ni	**Cr**	**Ti**	**Nb**	**Al**	**Fe**	**W**	**Mo**	**Co**	**Ta**	**N**	**O**	**C**
β-NiAl	64.6	5.0	2.2	-	21.2	-	-	-	7.0	-	-	-	-
β-NiAl-2	56.1	17.6	1.6	-	18.6	-	0.4	-	5.5	-	-	-	-
Ta-Ti-Nb carbide	16.9	2.0	15.4	11.3	5.6	-	-	-	2.0	32.1	-	-	14.7
Cr-Ni-Co phase	23.1	48.0	1.3	-	1.1	0.8	5.7	5.8	14.2	-	-	-	-
Cr-Ni-Co acicular phase	29.9	41.9	2.0	-	2.0	0.8	4.1	4.9	13.7	0.7	-	-	-
Matrix	64.7	15.07	3.9	0.6	4.2	-	1.8	1.0	7.7	1.0	-	-	-

Table A9. EDS analyses of some regions of the aluminized Inconel 738LC sample oxidized at 1000 °C (Figure 5e).

Region	Chemical Composition (Weight %)										
	Ni	**Cr**	**Ti**	**Nb**	**Al**	**W**	**Mo**	**Co**	**Ta**	**O**	**C**
Al_2O_3	2.8	0.9	-	-	48.2	-	-	-	-	48.1	-
β-NiAl	62.1	9.6	1.9	0.1	18.3	0.2	0.3	7.3	0.2	-	-
Ni-Al-Co-Ti phase	72.7	2.9	4.7	0.8	8.5	0.9	0.2	7.1	2.2	-	-
Ta-Ti-Nb-Ni carbide	9.8	3.7	23.1	11.4	1.0	6.9	3.1	1.7	26.5	-	12.8
Cr-Ni-Co-W-Mo phase	17.3	42.1	0.5	0.2	0.6	12.3	11.2	14.9	0.9	-	-
Ni-Cr-Co-Ti acicular phase	66.9	7.9	5.1	0.9	6.5	1.7	1.3	7.6	2.1	-	-
Matrix	52.5	27.9	1.4	0.1	2.1	2.3	1.9	11.5	0.3	-	-

Table A10. EDS analyses of some regions of the aluminized Inconel 738LC sample oxidized at 1050 °C (Figure 5f).

Region	Chemical Composition (Weight %)												
	Ni	**Cr**	**Ti**	**Nb**	**Al**	**Fe**	**W**	**Mo**	**Co**	**Ta**	**N**	**O**	**C**
Al_2O_3	-	-	0.4	-	55.2	-	-	-	-	-	-	44.4	-
β-NiAl	67.7	4.5	1.6	-	18.7	-	-	-	7.5	-	-	-	-

Table A10. *Cont.*

Region	Chemical Composition (Weight %)												
	Ni	**Cr**	**Ti**	**Nb**	**Al**	**Fe**	**W**	**Mo**	**Co**	**Ta**	**N**	**O**	**C**
Ta-Ti-Nb carbide	3.5	0.8	28.0	17.1	-	-	-	2.4	-	33.9	-	-	14.3
Cr carbide	5.1	72.7	0.4	-	-	-	7.7	5.9	2.1	-	-	-	6.1
Matrix	68.6	8.2	4.1	0.6	6.8	-	1.7	0.8	8.1	1.1	-	-	-

References

1. Krueger, D.D. The Development of Direct Age 718 for Gas Turbine Engine Disk Applications. In *Superalloys 718 Metallurgy and Applications*; The Minerals, Metals & Materials Society: Pittsburgh, PA, USA, 2012; pp. 279–296. [CrossRef]
2. Greene, G.A.; Finfrock, C.C. Oxidation of Inconel 718 in air at high temperatures. *Oxid. Met.* **2001**, *55*, 505–521. [CrossRef]
3. Zielińska, M.; Sieniawski, J.; Yavorska, M.; Motyka, M. Influence of chemical composition of nickel based superalloy on the formation of aluminide coatings. *Arch. Metall. Mater.* **2011**, *56*, 193–197. [CrossRef]
4. Inceyer, A.A.; Güven, G.; Demiralay, K.; Zeytin, H.K.; Usta, M. The Effects of Chemical Vapor Aluminizing Process Time and Post-processing for Nickel Aluminide Coating on CMSX-4 Alloy. *J. Mater. Eng. Perform.* **2021**, *31*, 2341–2353. [CrossRef]
5. Doremus, R.H. Diffusion in alumina. *J. Appl. Phys.* **2006**, *100*, 101301. [CrossRef]
6. Döleker, K.M.; Erdogan, A.; Yener, T.; Karaoglanlı, A.C.; Uzun, O.; Gök, M.S.; Zeytin, S. Enhancing the wear and oxidation behaviors of the Inconel 718 by low temperature aluminizing. *Surf. Coat. Technol.* **2021**, *412*, 127069. [CrossRef]
7. Shirvani, K.; Saremi, M.; Nishikata, A.; Tsuru, T. The role of silicon on microstructure and high temperature performance of aluminide coating on superalloy In-738LC. *Mater. Trans.* **2002**, *43*, 2622–2628. [CrossRef]
8. Koech, P.K.; Wang, C.J. High-Temperature Corrosion Behaviour of Aluminized-Coated and Uncoated Alloy 718 Under Cyclic Oxidation and Corrosion in NaCl Vapour at 750 °C. *Oxid. Met.* **2018**, *90*, 713–735. [CrossRef]
9. Kalaycı, T. Sıcak Daldırma Yöntemiyle Aluminyum Kaplanmış Inconel 718 Süperalaşımının Oksidasyon Direncinin İncelenmesi. Master's Thesis, Istanbul Technical University, Istanbul, Turkey, 2018. (In Turkish).
10. Bai, C.-Y.; Luo, Y.-J.; Koo, C.-H. Improvement of high temperature oxidation and corrosion resistance of superalloy IN-738LC by pack cementation. *Surf. Coat. Technol.* **2004**, *183*, 74–88. [CrossRef]
11. *SAE Standard AMS5662M*; SAE International Material Specification, Nickel Alloy, Corrosion and Heat-Resistant, Bars, Forgings, and Rings 52.5Ni-19Cr-3.0Mo-5.1Cb (Nb)-0.90Ti-0.50Al-18Fe Consumable Electrode or Vacuum Induction Melted 1775 °F (968 °C) Solution Heat Treated, Precipitation-Hardenable. SAE International: Warrendale, PA, USA, 2009.
12. Crystal Impact. *Match!: Phase Identification from Powder Diffraction Data*, Version 4.6, [Computer software]; Crystal Impact GbR: Bonn, Germany, 2025. Available online: https://www.crystalimpact.com/match/ (accessed on 8 November 2025).
13. Bouchaud, B.; Balmain, J.; Pedraza, F. Cyclic and Isothermal Oxidation at 1100 °C of a CVD Aluminised Directionally Solidified Ni Superalloy. *Oxid. Met.* **2008**, *69*, 193–210. [CrossRef]
14. Li, Z.; Wu, K.; Cao, J.; Wang, Y. Controlled synthesis of α-Al_2O_3 via the hydrothermal-pyrolysis method. *IOP Conf. Ser. Mater. Sci. Eng.* **2017**, *207*, 012004. [CrossRef]
15. Caplan, D.; Cohen, M. The Volatilization of Chromium Oxide. *Electrochem. Soc.* **1961**, *108*, 438. [CrossRef]
16. Sarraf, S.; Soltanieh, M.; Rastegari, S. Isothermal oxidation performance at 1000 °C of two different aluminide coatings deposited by the reactive air aluminizing (RAA) method on a nickel-based superalloy (IN738LC). *J. Alloys Compd.* **2025**, *1010*, 178123. [CrossRef]

Disclaimer/Publisher's Note: The statements, opinions and data contained in all publications are solely those of the individual author(s) and contributor(s) and not of MDPI and/or the editor(s). MDPI and/or the editor(s) disclaim responsibility for any injury to people or property resulting from any ideas, methods, instructions or products referred to in the content.